Real-Time Volumetric Imaging System for CMUT Arrays

Jung Woo Choe, Ömer Oralkan, Amin Nikoozadeh, Anshuman Bhuyan, Byung Chul Lee, Mustafa Gencel, and Butrus T. Khuri-Yakub

Edward L. Ginzton Laboratory, Stanford University, Stanford, CA

choejw@stanford.edu

***Abstract*—We designed and implemented a flexible real-time volumetric ultrasound imaging system for capacitive micromachined ultrasonic transducer (CMUT) arrays, consisting of an ultrasound data acquisition system, an FPGA board, and a host PC. The system works with arbitrary-shaped CMUT arrays and non-standard beamforming methods, as well as with regular-shaped CMUT arrays and conventional beamforming methods. In this paper, we present the system design and real-time imaging results obtained using this system with a ring array, a rectangular array, and a linear array. In synthetic phased array (SPA) imaging with a 64-element ring array, we could display 3 image planes with a total of about 70,000 pixels in real time, at a frame rate of 9 frames per second (fps) which was limited by the computational load on the CPU required for synthetic beamforming. On the other hand, the frame rate in classic phased array (CPA) imaging is limited by the data transfer time. In CPA imaging with a 16×16-element rectangular array, a frame rate of 5.4 fps was achieved for 1,250 acquisitions per frame and a 2.5-cm imaging depth. The frame rate can be increased by reducing the number of pixels processed in SPA, or by reducing the number of beams received in CPA, at the expense of degraded image quality or reduced field of view.**

Keywords- CMUT; Real-time imaging; Volumetric imaging; Ring array; 2-D array;

I. Introduction

One of the advantages capacitive micromachined ultrasonic transducers (CMUTs) have over piezoelectric transducers is in the fabrication of arrays with a large number of elements or with an arbitrary geometry [1]. As a result, various types of CMUT arrays with different geometry have been successfully fabricated [2]–[6]. Fig. 1 shows some of the CMUT arrays we fabricated recently. Another advantage of CMUTs is in the convenient integration with front-end electronics [1]. Each of the CMUT arrays in Fig. 1 has its own dedicated front-end electronics packaged in an application-specific integrated circuit (ASIC) and very closely integrated with the transducers [2]–[6]. Some of these ASICs contain only signal conditioning circuitry for buffering the received signals, while the others also include more complex circuitry to transmit pulses and perform transmit beamforming.

Conventional ultrasound imaging systems are designed for standard transducer arrays with regular geometry and simple front-end electronics, and are not suitable for probes with non-standard aperture geometry or customized front-end electronics. The objective of our imaging system is to perform real-time imaging with various CMUT probes with different geometry and different front-end electronics, and demonstrate volumetric imaging for probes with 2-dimensional apertures, such as ring arrays and rectangular arrays. Multiple beamforming methods, including classic phased array (CPA), synthetic phased array (SPA), and plane-wave compounding, should be available because the optimal beamforming method for real-time imaging differs from probe to probe, depending on the aperture geometry and the number of elements in the array, and from application to application. In addition, we plan to use this imaging system in photoacoustic imaging as well.

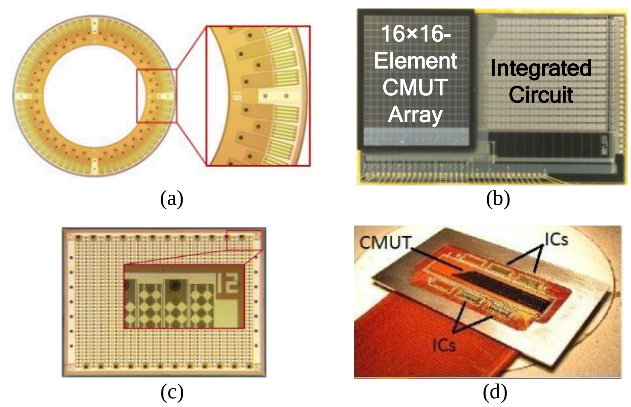

Figure 1. Various CMUT arrays with different geometry and electronics. (a) 64-element ring array (b) 16×16-element rectangular array (c) 24-element micro-linear array (d) 132-element linear array

We describe the overall system design and the important system components in Section II, and some of the imaging results obtained using this system are presented in Section III. In Section IV, we briefly discuss the frame rate and the system tradeoffs.

II. System Design

The system consists of an ultrasound data acquisition system (Verasonics data acquisition system, Verasonics, Inc., Redmond, WA), a host PC (Mac Pro, Apple Inc., Cupertino, CA), an FPGA board (Virtex-6 FPGA ML605, Xilinx Inc., San Jose, CA), a laser (Surelite OPO Plus, Continuum, Santa Clara, CA), and a custom-designed interface PCB. The top-level architecture of the overall system is shown in Fig. 2.

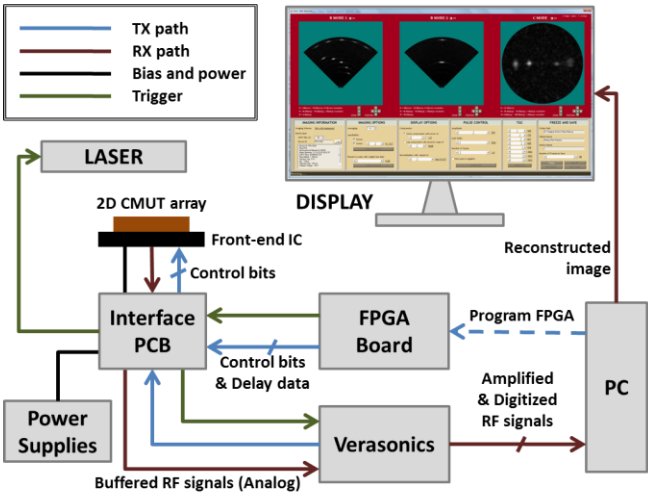

Figure 2. Top-level architecture of the system.

The Verasonics data acquisition system acquires the RF data received by the transducers and pre-amplified by the front-end electronics. It has 128 transmit channels and 64 receive channels that we can program using Matlab scripts. The acquired data are transferred, via an 8-lane PCI express (PCIe) interface at a 1.2-GB/s transfer rate, to the host PC, on which our custom software developed in C++ runs to reconstruct images and display them on the screen in real-time. The host PC has 16-GB RAM, two quad-core (8 virtual cores with hyper-threading) 3-GHz CPUs (Intel Xeon Processor X5570, Intel Corporation, Santa Clara, CA), and a GPU (GeForce GTX 285, Nvidia, Santa Clara, CA). Currently the software runs only on CPU, and the next version of software that utilizes GPU is now under development.

Different options are available for transmit. In the simplest cases where the front-end electronics just performs signal conditioning and pre-amplification of received signals, the pulsers in the Verasonics system can be used to transmit pulses. For the probes with their own pulsers in the front-end IC, we program the FPGA to generate transmit delay data and control the on-chip pulsers for transmit beamforming. The delay data, quantized with a 20-ns resolution, are loaded into the front-end IC at a 50-MHz rate, resulting in a 2.56-µs loading time per beam. In photoacoustic imaging, the laser is used for excitation instead of pulsers. When the Verasonics transmitters are not used, we run the Verasonics in the external trigger mode to use it as a receiver and sample the raw data received by transducers.

The individual system components are connected together by the custom-designed interface PCB, which also provides an interface to CMUT probes and power supplies. For synchronization of the system components, the FPGA generates and distributes clock and trigger signals.

III. Imaging Results

A. *Ring Array Imaging*

Multiple imaging methods, including flash, CPA, SPA, SPA-W (SPA with aperture weighting), SPA-H (SPA with Hadamard coding), and SPA-HW (SPA with both aperture weighting and Hadamard coding), were tested for real-time

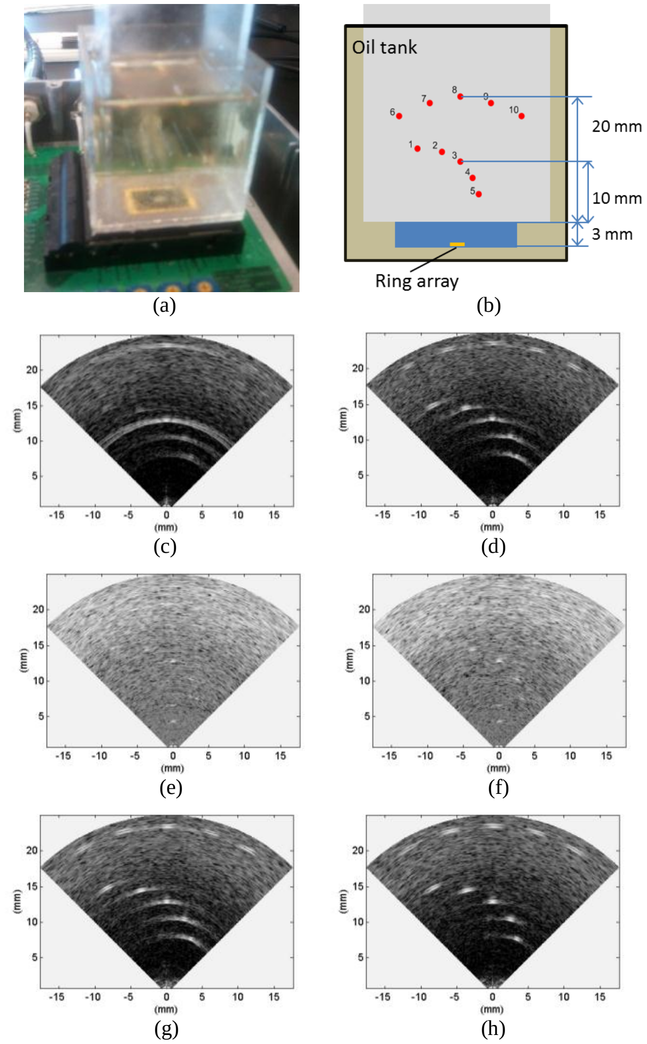

Figure 3. B-mode images of a phantom with 10 fishing wires, for six different imaging methods with a ring array, shown in 40-dB dynamic range. (a) Picture of the phantom in an oil tank (b) Location of each wire target (c) Flash (d) CPA (e) SPA (f) SPA-W (g) SPA-H (h) SPA-HW

volumetric imaging with a 64-element ring array [Fig. 1 (a)]. In flash imaging, only one beam is transmitted in each frame without any delay. It is the fastest imaging method, but has a poor image resolution, especially in off-axis region because the beam is self-focused along the axis due to the circular symmetry of the ring geometry. CPA achieves a good resolution and a good SNR. However, it requires a large number of beams to sample the entire volume of interest without undersampling, resulting in a very slow frame rate and a need for immense memory space. In addition, due to the absence of transducer elements in the center of the ring, this method has a problem with high sidelobes. Using SPA, we can obtain an excellent beam profile with dynamic focusing in both transmit and receive, hence an excellent resolution, with a number of firings as small as the number of elements. SPA suffers from a low SNR, but it can be overcome by spatial pulse-encoding technique such as Hadamard coding [7], [8]. Another advantage of SPA is that we can apply an aperture weighting scheme to obtain an effective full-disk aperture, for improved beam profile with lower sidelobes [9], [10].

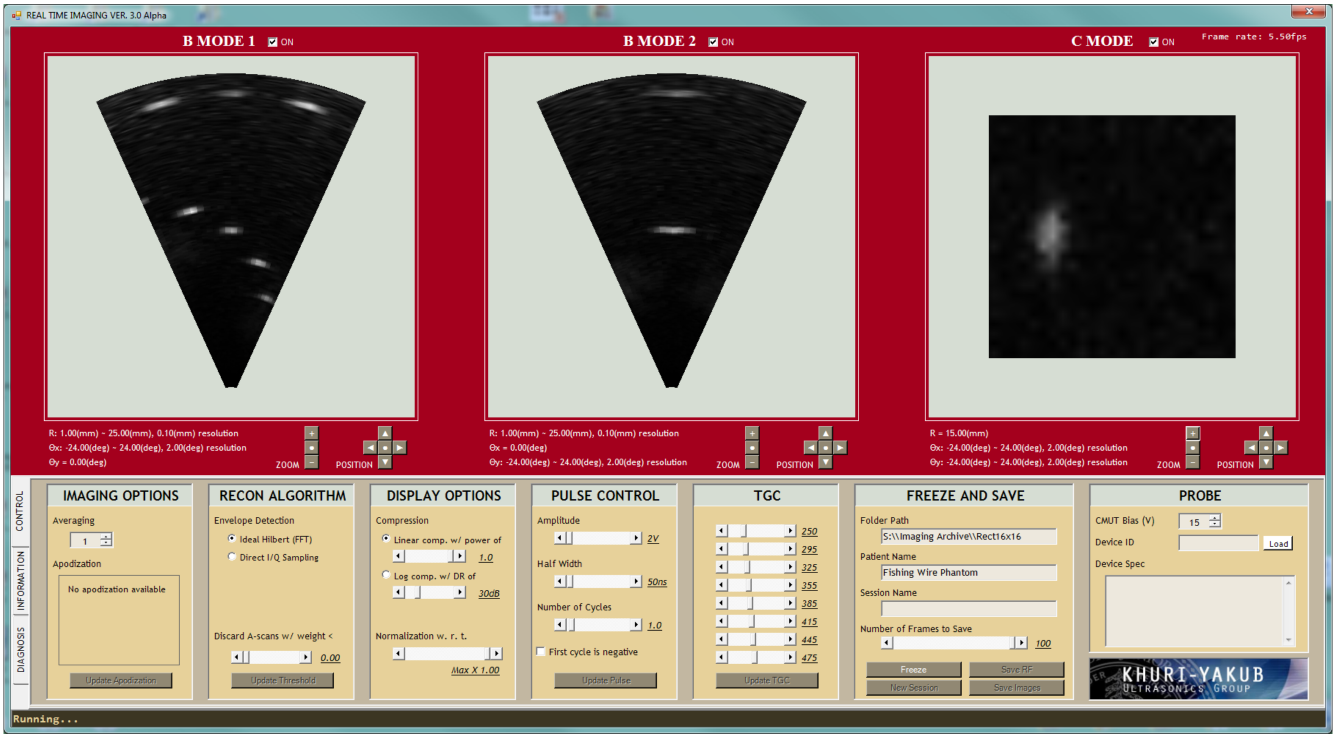

Figure 4. The custom software user interface, and real-time images of the fishing wire phantom, obtained with a 16×16-element rectangular array, using 625 focused beams. For transmit, we used unipolar pulses from the on-chip pulsers with 25-V amplitude and single cycle. The numbers in the Pulse Control panel are not used when the pulses are transmitted from the on-chip pulsers.

Fig. 3 presents B-mode images of an experimental phantom with 10 fishing wires, obtained using the six different imaging methods. From these experiments, we concluded that SPA-HW is the best option for real-time volumetric imaging with a ring array, which gives a good SNR, an excellent resolution, and a satisfactory frame rate. Using SPA-HW, we could achieve a frame rate of about 10 frames per second (fps) while displaying 3 image planes, two B-mode planes perpendicular to each other and one constant-depth image, in real-time. More discussion on the frame rate follows in Section IV.

B. Rectangular Array Imaging

The CMUT rectangular array we used in the experiment consists of 256 transducer elements [Fig. 1 (b)]. The front-end IC contains 256 pulsers and transmit beamforming circuitry, but has only 16 receive channels. A receive channel is shared between the 16 elements on the same column, and only 16 elements can receive simultaneously at each acquisition. So, instead of receiving from the full aperture, we used only 32 diagonal elements for receive [11], by transmitting every beam twice and receiving from one of the two diagonals at each acquisition. The on-chip pulsers and the transmit beamforming circuitry are controlled by the FPGA, which also selects the receiving elements in each acquisition.

We used CPA with 625 focused beams generated by the on-chip transmit circuitry to sample the volume of interest. The maximum number of acquisitions per frame is restricted by the Verasonics sequencer memory, and we can transmit only up to 697 beams with two acquisitions per beam. To avoid spatial undersampling, the viewing angle was limited to 50° in the experiment. Fig. 4 shows the resulting real-time images of the same wire phantom as in the ring array imaging, along with the user interface of our custom-developed software. Here, the images are shown in linear scale without compression. With 625 beams and two acquisitions per beam, a 5.4-fps frame rate was achieved for displaying two B-mode images perpendicular to each other and one constant-depth image at 15-mm depth.

C. Linear Array Imaging

Real-time imaging using the first 64 channels of a 132-element CMUT linear array with elevational focus at 11 mm [Fig. 1 (d)] was demonstrated. A human neck was imaged using CPA with 91 focused beams on the B-mode plane. With a frame rate of 46 fps, we could clearly see the jugular vein pulsating. A captured B-mode image is presented in Fig. 5.

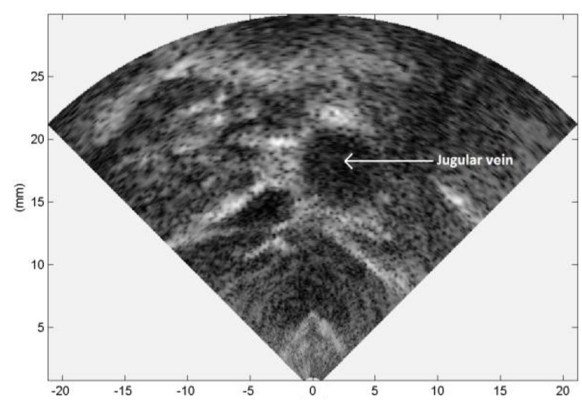

Figure 5. B-mode image of a human neck, shown in 45-dB dynamic range. Pulsating jugular vein is clearly seen in the real-time image with a 46-fps frame rate.

TABLE I. FRAME RATES OF CPA WITH A RECTANGULAR ARRAY

Number of beams[1]	625	182	92	62
Frame rate[2]	5.4	19	37	54

[1]Each beam was transmitted twice to receive from both diagonals.
[2]Frame rates are in frames per second (fps).

TABLE II. FRAME RATES OF SPA WITH A RING ARRAY

Number of pixels per plane	22,801 (High resolution)			11,201 (Low resolution)		
Number of planes	3	2	1	3	2	1
Using 4,096 A-scans[1]	9	12	20	17	21	28
Using 1,560 A-scans[2]	20	26	35	32	38	45

[1]Using all the A-scans from 64 transmit and 64 receive elements
[2]Discarding 2,536 A-scans with a weight less than 0.5 after aperture weighting
[1,2]Frame rates are in frames per second (fps).

IV. SYSTEM TRADEOFFS

Other than the ultrasound time of flight, the imaging system imposes practical limitations on real-time imaging performance. The data obtained using the Verasonics data acquisition system are transferred to the host PC for image reconstruction via an 8-lane PCIe interface. The data transfer rate, which is limited by the PCIe to local bus translator chip (PEX 8311, PLX Technology, Sunnyvale, CA), is 1.2 GB/s, a rate that is 4.8 times slower than the data acquisition assuming 45-MHz data sampling. Therefore, in all imaging methods, the data transfer rate from the Verasonics data acquisition system to the host PC limits the achievable frame rate, and in many cases, including CPA, this is the actual bottleneck determining the frame rate. To alleviate this limitation and increase the frame rate, the amount of data transferred should be reduced, either by decreasing the imaging depth, or by reducing the number of data acquisitions per frame. Table I shows the experimental frame rates with different number of beams in CPA imaging, under the same imaging depth of 25 mm with 5-MHz transducers and 22.5-MHz sampling frequency. With fewer beams, the frame rate increases linearly, but at the cost of degraded image quality.

In synthetic imaging, where the amount of computation is very large, the computational load required for image reconstruction exceeds the overhead in data transfer, and limits the frame rate further. Thus, to increase the frame rate of SPA, the amount of computation should be reduced by decreasing the number of pixels processed or the number of A-scans used in the delay-and-sum operations, as shown in Table II. The computation speed can be improved by upgrading hardware, for example, using more number of CPU cores or using a GPU with many parallel cores in the computation [12].

V. CONCLUSION AND FUTURE WORK

We designed and implemented a real-time volumetric imaging system that works with various types of CMUT probes with different geometry and different electronics. The system is capable of real-time imaging with multiple beamforming techniques, including non-standard methods as well as conventional methods. Real-time imaging using this system with a ring array, a rectangular array, and a linear array were demonstrated.

To improve the frame rate in synthetic imaging, we are currently developing new imaging software that performs image reconstruction on GPU platform for faster computation. Also, we are now working on real-time volumetric imaging for larger rectangular arrays, with 32×32 and 64×64 elements.

ACKNOWLEDGMENT

This work is funded by the National Institute of Health under grants HL67647 and CA134720. Xilinx and Nvidia generously donated the FPGA board and GPU, respectively. We would like to thank Verasonics, Inc. for providing technical support. We also thank the Stanford Nanofabrication Facility for CMUT fabrication, and National Semiconductor (Texas Instrument) for IC fabrication.

REFERENCES

[1] Ö. Oralkan, A. S. Ergun, J. A. Johnson, U. Demirci, M. Karaman, K. Kaviani, T. H. Lee, and B. T. Khuri-Yakub, "Capacitive micromachined ultrasonic transducers: Next-generation arrays for acoustic imaging?," *IEEE Trans. Ultrason., Ferroelect., Freq. Contr.*, vol. 49, no. 11, pp. 1596–1610, Nov. 2002.

[2] J. Knight, J. McLean, and F. L. Degertekin, "Low temperature fabrication of immersion capacitive micromachined ultrasonic transducers on silicon and dielectric substrates," *IEEE Trans. Ultrason., Ferroelect., Freq. Contr.*, vol. 51, no. 10, pp. 1324–1333, Oct. 2004.

[3] A. Nikoozadeh, I. O. Wygant, D. Lin, Ö. Oralkan, A. S. Ergun, D. N. Stephens, K. E. Thomenius, A. M. Dentinger, D. Wildes, G. Akopyan, K. Shivkumar, A. Mahajan, D. J. Sahn, and B. T. Khuri-Yakub, "Forward-looking intracardiac ultrasound imaging using a 1-D CMUT array integrated with custom front-end electronics," *IEEE Trans. Ultrason., Ferroelect., Freq. Contr.*, vol. 55, no. 12, pp. 2651–2660, Dec. 2008.

[4] A. Nikoozadeh, Ö. Oralkan, M. Gencel, J. W. Choe, D. N. Stephens, A. de la Rama, P. Chen, K. Thomenius, A. Dentinger, D. Wildes, K. Shivkumar, A. Mahajan, M. O'Donnell, D. Sahn, and P. T. Khuri-Yakub, "Forward-looking volumetric intracardiac imaging using a fully integrated CMUT ring array," in *Proc. IEEE Ultrason. Symp.*, pp. 511–514, 2009.

[5] I. Wygant, X. Zhuang, D. Yeh, Ö. Oralkan, A. S. Ergun, M. Karaman, and B. T. Khuri-Yakub, "Integration of 2D CMUT arrays with front-end electronics for volumetric ultrasound imaging," *IEEE Trans. Ultrason., Ferroelect., Freq. Contr.*, vol. 55, no. 2, pp. 327–342, Feb. 2008.

[6] I. O. Wygant, N. S. Jamal, H. J. Lee, A. Nikoozadeh, Ö. Oralkan, M. Karaman, and B. T. Khuri-Yakub, , "An integrated circuit with transmit beamforming flip-chip bonded to a 2-D CMUT array for 3-D ultrasound imaging," *IEEE Trans. Ultrason., Ferroelect., Freq. Contr.*, vol. 56, no. 10, pp. 2145–56, , Oct. 2009.

[7] R. Y. Chiao, L. J. Thomas, and S. D. Silverstein, "Sparse array imaging with spatially-encoded transmits," in *Proc. IEEE Ultrason. Symp.*, vol. 2, pp. 1679–1682, 1997.

[8] T. X. Misaridis and J. A. Jensen, "Space-time encoding for high frame rate ultrasound imaging," *Ultrasonics*, vol. 40, pp. 593–597, May 2002.

[9] S. J. Norton, "Annular array imaging with full-aperture resolution," *J. Acoust. Soc. Am.*, vol. 92, no. 6, pp. 3202–3206, Dec. 1992.

[10] S. J. Norton, "Synthetic aperture imaging with arrays of arbitrary shape. Part II: The annular array," *IEEE Trans. Ultrason., Ferroelect., Freq. Contr.*, vol. 49, pp. 404–408, Apr. 2002.

[11] M. Karaman, I. O. Wygant, Ö. Oralkan, and B. T. Khuri-Yakub, "Minimally redundant 2-D array designs for 3-D medical ultrasound imaging ," *IEEE Trans. Medical Imaging*, vol. 28, no. 7, pp. 1051–1061, Jul. 2009.

[12] B. Yiu, I. Tsang, and A. Yu, "Real-time GPU-based software beamformer designed for advanced imaging methods research," in *Proc. IEEE Ultrason. Symp.*, pp. 1920–1923, 2010.